

K-edge subtraction vs. A-space processing for x-ray imaging of contrast agents: SNR

Robert E. Alvarez[‡]

Purpose: To compare two methods that use x-ray spectral information to image externally administered contrast agents: K-edge subtraction and basis-function decomposition (the A-space method),

Methods: The K-edge method uses narrow band x-ray spectra with energies infinitesimally below and above the contrast material K-edge energy. The A-space method uses a broad spectrum x-ray tube source and measures the transmitted spectrum with photon counting detectors with pulse height analysis. The methods are compared by their signal to noise ratio (SNR) divided by the patient dose for an imaging task to decide whether contrast material is present in a soft tissue background. The performance with iodine or gadolinium containing contrast material is evaluated as a function of object thickness and the x-ray tube voltage of the A-space method.

Results: For a tube voltages above 60 kV and soft tissue thicknesses from 5 to 25 g/cm², the A-space method has a larger SNR per dose than the K-edge subtraction method for either iodine or gadolinium containing contrast agent.

Conclusion: Even with the unrealistic spectra assumed for the K-edge method, the A-space method has a substantially larger SNR per patient dose.

Key Words: spectral x-ray, K-edge subtraction, basis decomposition, contrast agent, photon counting,

1. INTRODUCTION

K-edge subtraction was one of the first methods to use x-ray spectral information to improve the visibility of contrast agents injected into the body^{2,3,4}. An alternative method utilizing spectral information is the basis decomposition method⁵ (the A-space method). Alvarez⁶ showed this method can be used to provide near optimal signal to noise ratio (SNR)⁷ with low energy-resolution measurements. Although both methods use spectral information, they are quite different and an interesting question is which one provides a better SNR per dose for detecting an externally administered contrast agent in a soft tissue background?

This paper examines that question for idealized spectra and detectors. For K-edge subtraction, monoenergetic spectra with energies just below and above the K-edge energy and a quantum noise-limited, negligible pileup photon counting detector are used. For the A-space method, a broad spectrum x-ray tube source is used with an ideal photon counting detector with pulse height analysis (PHA).

The imaging task is to detect contrast material embedded in soft tissue. The signal to noise ratios of the two methods are compared for equal dose, which is approximated as the absorbed energy. Since, in general, the square of the SNR is proportional to dose, the parameter compared is $SNR^2/Dose$. This parameter is computed as a function of soft-tissue object thickness and the x-ray tube voltage for contrast agents containing iodine or gadolinium.

The imaging task does not measure the full capa-

*ralvarez@aprendtech.com

[†]Code for figures available online¹

bility of either method. The A-space method extracts a great deal more information about the object than simply the presence of the contrast agent^{8,9,10}. The K-edge subtraction method can discriminate against body materials with different compositions so long as their attenuation coefficient is continuous at the K-edge energy. Nevertheless the imaging task used allows us to directly compare the fundamental performance of the two methods for an important clinical application. More general comparisons including the presence of other body materials and practical limitations on the x-ray source spectra for the K-edge subtraction method are under research.

Recent examples of work in this area include Roessl and Proksa¹¹, who applied the A-space method to image contrast agents as did Zimmerman and Schmidt¹². Dilmanian et al.¹³ used a synchrotron radiation source at a nuclear physics laboratory to image contrast agents with K-edge subtraction. Shikhaliev¹⁴ pre-filtered a broad spectrum source with high atomic number materials to provide a bi-modal spectrum. The filtered transmitted spectrum was measured with a photon counting detector with PHA and the SNR of the contrast material thickness was computed. None of these papers compared the K-edge subtraction method to the A-space method directly.

2. METHODS

In this section, the imaging task for the signal to noise ratio definition is described. Then expressions for the SNR and absorbed energy with the K-edge subtraction and A-space methods are derived. Finally, the SNR per absorbed energy is computed as a function of the object thickness and the tube voltage for contrast agents containing iodine or gadolinium.

2.A. The imaging task

The imaging task assumes the object shown in Fig. 2.1. The task decides whether a contrast material is present from measurements of the transmitted x-ray

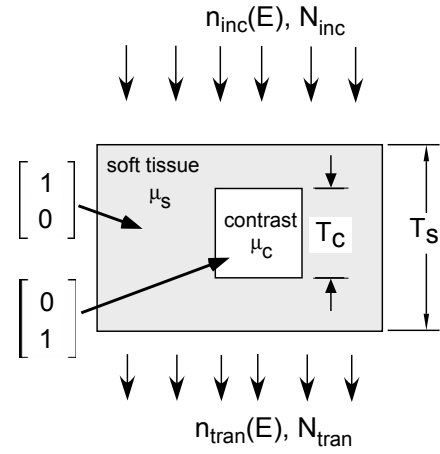
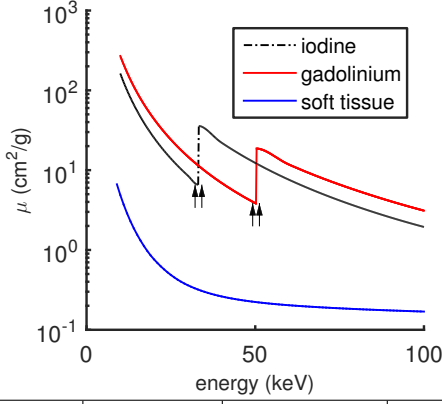


Figure 2.1: The imaging task is to detect the presence of an externally administered contrast agent from measurements of the transmitted energy spectrum, $n_{tran}(E)$, where E is the x-ray energy. The incident spectrum is $n_{inc}(E)$ and the total number of incident photons is $N_{inc} = \int n_{inc}(E)dE$. The soft tissue material has attenuation coefficient $\mu_s(E)$ and thickness T_s , while the contrast material has attenuation coefficient $\mu_c(E)$ and thickness T_c . For A-space processing, a basis set consisting of the background and contrast materials' attenuation coefficients is used. With this basis set, the coefficients, the a vectors, for the soft tissue is $[0, 1]^T$ and the contrast material $[1, 0]^T$ as shown in the figure. Column vectors are used and the symbol T denotes the transpose.

energy spectrum.

Assuming normally distributed noise, the probability of error depends only on the signal to noise ratio¹⁵, where the signal is the square of the difference in the expected values of the measurements between the soft tissue only and the soft tissue plus contrast materials and the noise is the variance of the measurements. The contrast material thickness will be assumed to be sufficiently small that the variance is essentially the same in the soft tissue-only and the contrast regions.



| | E_K (keV) | $\mu(E_{K-})$ (cm²/g) | $\mu(E_{K+})$ (cm²/g) |
|-------------------|----------------|--------------------------|--------------------------|
| iodine | 33.17 | 10.18 | 31.59 |
| gadolinium | 50.24 | 4.88 | 14.55 |

Figure 2.2: X-ray attenuation coefficients of the high atomic number elements used in contrast agents as a function of x-ray energy. The attenuation coefficient of soft tissue is also plotted for comparison. The table shows the K-edge energy and the attenuation coefficients just below and above it for iodine and gadolinium.

2.B. Ideal K-edge subtraction

Figure 2.2 shows the attenuation coefficients of iodine and gadolinium as well as soft tissue. Notice the sharp discontinuities of the coefficients of the contrast materials. The absorption edge energies are unique to each element. The energies and the attenuation coefficients just above and below the discontinuities are shown in the table in the figure. Soft tissue and other biological materials have attenuation coefficients that are continuous throughout the diagnostic energy range.

For the ideal K-edge method, we use delta function x-ray spectra with energies just below and just above the K-edge energy, E_{k-} and E_{k+} , and compute the difference of the logarithm of the number of transmitted photons. Referring to Fig. 2.1, the expected values of the transmitted photon counts with the two spectra are N_{K-} and N_{K+}

$$\begin{aligned} N_{K-} &= (N_0/2) e^{-\mu_s(E_{k-})(t_s-t_c)-\mu_c(E_{k-})t_c} \\ N_{K+} &= (N_0/2) e^{-\mu_s(E_{k+})(t_s-t_c)-\mu_c(E_{k+})t_c} \end{aligned} \quad (2.1)$$

In this equation, N_0 is the sum of the incident photons of both spectra, $\mu_s(E)$ is the soft-tissue attenuation coefficient at x-ray energy E , t_s is the soft tissue material thickness, $\mu_c(E)$ is the contrast material attenuation coefficient, and t_c its thickness. The incident photons were divided equally between the two spectra.

The K-edge signal S_K is the difference of the logarithms of the photon counts

$$S_K = \log(N_{K-}) - \log(N_{K+}). \quad (2.2)$$

Using Equations 2.1, this signal is

$$\begin{aligned} S_K &= [\mu_s(E_{k+}) - \mu_s(E_{k-})](t_s - t_c) + \dots \\ &\quad [\mu_c(E_{k+}) - \mu_c(E_{k-})]t_c. \end{aligned} \quad (2.3)$$

In the background region, the contrast material thickness is zero, $t_c = 0$, and the background material thickness is $t_s = T_s$ so the signal is

$$S_{Kb} = T_s [\mu_s(E_{k+}) - \mu_s(E_{k-})]. \quad (2.4)$$

Since the soft tissue attenuation coefficient function $\mu_s(E)$ is continuous, the K-edge subtraction background region signal can be made arbitrarily small by using measurement energies sufficiently close to the K-edge energy E_k

$$\begin{aligned} E_{k-}, E_{k+} &\rightarrow E_k \\ \mu_s(E_{k-}) &\rightarrow \mu_s(E_{k+}) \\ S_{Kb} &\rightarrow 0 \end{aligned} \quad (2.5)$$

In the contrast material region, the background material thickness is $T_s - T_c$ and the contrast thickness is T_c so the K-edge signal from Eq. 2.3 is

$$\begin{aligned} S_{Kc} &= [\mu_s(E_{k+}) - \mu_s(E_{k-})](T_s - T_c) + \dots \\ &\quad [\mu_c(E_{k+}) - \mu_c(E_{k-})]T_c. \end{aligned} \quad (2.6)$$

For the ideal energies specified in Eq. 2.5, the first term is essentially zero so the signal in the contrast region is

$$S_{Kc} = [\mu_c(E_{k+}) - \mu_c(E_{k-})]T_c. \quad (2.7)$$

The probability distributions of the photon counts in Equations 2.1 can be modeled as independent Poisson since they are measured with different spectra. The variance of the logarithm of a Poisson random variable with expected value $\langle n \rangle$ is $1/\langle n \rangle$ ⁶. Therefore, the variance of the K-edge signal, which is the difference of their logarithms, Eq. 2.3, is the sum of the variances of the logarithms of the individual counts

$$\text{Var}(S_K) = \frac{1}{\langle N_{K-} \rangle} + \frac{1}{\langle N_{K+} \rangle}. \quad (2.8)$$

The expected values are sufficiently large that we can use the normal approximation to the Poisson¹⁶.

2.C. A-space processing

The A-space method⁵ approximates the attenuation coefficient at points within the object as a linear combination of basis functions of energy multiplied by coefficients that depend on the position \mathbf{r} within the object.

$$\mu(\mathbf{r}, E) = a_1(\mathbf{r})\mu_1(E) + a_2(\mathbf{r})\mu_2(E). \quad (2.9)$$

To apply this method to the imaging task in Section 2.A, we use the attenuation coefficients of the soft tissue and contrast material, $\mu_s(E)$ and $\mu_c(E)$, as the basis functions^{6,17}. With this basis set, the vectors of the basis set coefficients of the soft tissue and contrast materials are $\mathbf{a}_s = [1 \ 0]^T$ and $\mathbf{a}_c = [0 \ 1]^T$. The superscript T denotes a transpose.

In general, we need a three function basis set to approximate the attenuation coefficients of biological materials and a high atomic number contrast agent accurately¹⁶. However, the two function set is sufficient to represent the materials in the object, which is assumed to be composed only of two materials, and it facilitates the comparison with the K-edge method.

The line integral of the attenuation coefficient along a line \mathcal{L} from the source to a detector pixel is

$$\int_{\mathcal{L}} \mu(\mathbf{r}, E) d\mathbf{r} = A_s \mu_s(E) + A_c \mu_c(E). \quad (2.10)$$

where $A_i = \int_{\mathcal{L}} a_i(\mathbf{r}) d\mathbf{r}$, $i = s, c$ and the superscript T denotes a matrix transpose. We summarize the line integrals as a vector $\mathbf{A} = [A_s \ A_c]^T$, the A-vector.

The A-space method estimates the A-vector^{5,18,19} from measurements of the transmitted spectra. A photon counting detector with pulse height analysis is used so the counts in each bin are a different spectrum measurement. Neglecting scatter and pulse pileup, the expected value of the count in PHA bin k is

$$\langle N_k(\mathbf{A}) \rangle = \int \Pi_k(E) n_{inc}(E) e^{-A_s \mu_s(E) - A_c \mu_c(E)} \quad (2.11)$$

where $n_{inc}(E)$ is the incident spectrum and $\Pi_k(E)$ is the idealized bin response for bin k , equal to 1 inside the bin and 0 elsewhere. The measurements can be summarized as a vector $\mathbf{L}(\mathbf{A})$ with components

$$\mathbf{L}_k(\mathbf{A}) = -\log \left(\frac{N_k(\mathbf{A})}{\langle N_k(0) \rangle} \right)$$

where $\langle N_k(0) \rangle$ is the expected values of the bin count with zero object thickness. The estimator inverts $\mathbf{L}(\mathbf{A})$ to compute the best estimate of the A-vector, $\hat{\mathbf{A}}$, given \mathbf{L} .

Since the measurements are random quantities, the A-vector estimates will also be random. If \mathbf{C}_A is their covariance, the signal to noise ratio for the imaging task is

$$\text{SNR}^2 = \delta \mathbf{A}^T \mathbf{C}_A^{-1} \delta \mathbf{A} \quad (2.12)$$

where $\delta \mathbf{A}$ is the difference of the A-vectors in the regions with and without contrast material and the superscript -1 denotes the matrix inverse. The optimal SNR is computed using the Cramér-Rao lower bound (CRLB), $\mathbf{C}_{A, \text{CRLB}}$, the minimum covariance for any unbiased estimator²⁰. For the number of photons required with material selective imaging, the CRLB is¹⁶

$$\mathbf{C}_{A, \text{CRLB}} = (\mathbf{M}^T \mathbf{C}_L^{-1} \mathbf{M})^{-1}. \quad (2.13)$$

In this equation, $\mathbf{M} = \partial \mathbf{L} / \partial \mathbf{A}$ and \mathbf{C}_L is the covariance of the \mathbf{L} measurements. With the assumptions of no pileup and a quantum noise limited detector, \mathbf{C}_L is a diagonal matrix with elements $C_{L, kk} = 1/\langle N_k \rangle$ and the

matrix \mathbf{M} has elements⁶

$$M_{ij} = \frac{\partial L_i}{\partial A_j} = \langle \mu_j(E) \rangle_{\hat{n}_i(E)}.$$

That is, each element is the effective value of basis function $\mu_j(E)$ in the normalized spectrum $\hat{n}_i(E)$

$$\hat{n}_i(E) = \frac{\Pi_i(E)n_{inc}(E)e^{-A_s\mu_s(E)-A_c\mu_c(E)}}{\int \Pi_i(E)n_{inc}(E)e^{-A_s\mu_s(E)-A_c\mu_c(E)}dE}.$$

Because we use the attenuation coefficients of the object materials as the basis functions, the \mathbf{A} -vector is

$$\mathbf{A} = t_s \mathbf{a}_s + t_c \mathbf{a}_c \quad (2.14)$$

where t_s and t_c are the thicknesses of the soft tissue and contrast materials. In the soft tissue only region,

$$\mathbf{A}_{\text{soft tissue}} = \begin{bmatrix} T_s \\ 0 \end{bmatrix}. \quad (2.15)$$

and in the region with contrast agent

$$\mathbf{A}_{\text{contrast}} = \begin{bmatrix} T_s - T_c \\ T_c \end{bmatrix} \quad (2.16)$$

so the difference vector is

$$\delta \mathbf{A} = \mathbf{A}_{\text{contrast}} - \mathbf{A}_{\text{no contrast}} = T_c \begin{bmatrix} -1 \\ 1 \end{bmatrix}.$$

Using Eq. 2.12, the optimal SNR with the A-space method is

$$SNR_{opt}^2 = T_c^2 [1, -1] \mathbf{M}^T \mathbf{C}_L^{-1} \mathbf{M} \begin{bmatrix} -1 \\ 1 \end{bmatrix}.$$

2.D. Absorbed energy

The spectra for the K-edge subtraction and A-space processing are different so in order to compare the two methods on an equal basis we need a way to normalize their SNR. The method used is to divide the SNR by the x-ray energy absorbed in the object, which is used as a proxy for the x-ray dose. The absorbed energy is computed from the energy absorption co-

efficient of the soft tissue material, $\mu_{abs,s}(E)$, which measures the energy absorbed by the object from the incident x-ray photons²¹. Assuming the contrast material is so thin that it does not absorb significantly, the absorbed energy is

$$Q_{abs} = Q_{inc} \left[1 - \int \hat{q}_{inc}(E) e^{-T_s \mu_{abs,s}(E)} dE \right]. \quad (2.17)$$

In this equation, the incident energy spectrum is $q_{inc}(E) = E n_{inc}(E)$, where $n_{inc}(E)$ is the photon number spectrum incident on the object. The energy spectrum $q_{inc}(E)dE$ gives the sum of energies of the photons from E to $E + dE$. The normalized energy spectrum is

$$\hat{q}_{inc}(E) = \frac{q_{inc}(E)}{\int q_{inc}(E)dE}.$$

where the denominator is the total energy of the incident photons

$$Q_{inc} = \int q_{inc}(E)dE.$$

For the A-space method, the absorbed energy is given by Eq. 2.17 with the incident x-ray tube spectrum $n_{inc}(E)$ calculated with the TASMIP algorithm²².

For the idealized K-edge method described in Section 2.B, the two delta function spectra are assumed to be arbitrarily close to the K-edge energy, E_K , with a total number of photons for both spectra equal to N_0 . With these assumptions, the absorbed energy is

$$Q_{abs,K} = N_0 E_K \left[1 - e^{-T_s \mu_{abs,s}(E_K)} \right]. \quad (2.18)$$

2.E. SNR per absorbed energy as a function of object thickness

To compare the methods, the SNR^2 divided by the absorbed energy was computed as a function of the soft-tissue material thickness from 5 to 25 g/cm^2 . Contrast agents with iodine or gadolinium as the high atomic number element were used. The contrast material thickness was fixed at $5 \times 10^{-3} g/cm^2$. The absorbed energies with the two methods was computed as described in Section 2.A.

For the K-edge method, delta function spectra with energies infinitesimally below and above the contrast material's K-edge energy were assumed as described in Section 2.B. The total incident photons were equally distributed between the two spectra.

For the A-space method, a 100 kV x-ray tube spectrum computed with the TASMIP algorithm²² was used with photon counting detectors with five PHA bins. The PHA bins were adjusted to give an equal number of photons per bin for the spectrum transmitted through 5 g/cm^2 of soft tissue. An efficient estimator with low bias and with A-vector noise covariance approximately equal to the CRLB was assumed.

2.F. SNR per absorbed energy as a function of tube voltage

The spectrum used with the A-space processing is controlled by the x-ray tube voltage so the SNR per dose was computed as a function of voltages from 40 to 100 kV. The object thickness was 20 g/cm^2 . For comparison, the SNR per dose of the K-edge method with this object thickness was also plotted.

3. RESULTS

3.A. SNR vs. object thickness

Figure 3.1 shows the SNR per dose as a function of the soft tissue thickness. Panel (a) is for an iodine containing contrast agent and Panel (b) for gadolinium containing contrast agent. In the panels, the SNR of the two methods are on the left and their ratio on the right. The tube voltage for the A-space method was 100 kV.

3.B. SNR vs. tube voltage

Figure 3.2 shows the SNR per absorbed energy as a function of the x-ray tube voltage. The left graph is for an iodine contrast agent and the right for gadolinium contrast. The K-edge method SNR per dose is also

plotted. Since it does not depend on the tube spectrum, it is a constant. The object thickness was fixed at 20 g/cm^2 .

4. DISCUSSION

Figure 3.1 shows that for soft tissue thickness from 5 to 25 g/cm^2 the A-space method's SNR per dose is larger than that of the K-edge subtraction method. The ratio of the SNR values with the two methods depends on the contrast agent. For iodine containing agents, the ratio becomes larger as the object thickness increases approaching a value of 9 at 25 g/cm^2 . The gadolinium ratio is approximately constant with a value approximately 3. The K-edge energy of iodine, 33.2 keV, is substantially lower than that of gadolinium, 50.2 keV, so the iodine K-edge signal is attenuated much more strongly as the object thickness increases.

Figure 3.2 shows that for tube voltages greater than 60 kV, the A-space method SNR is larger than the K-edge subtraction method SNR for both iodine and gadolinium. For iodine, the A-space method SNR is approximately 6 times larger than the K-edge subtraction value. For gadolinium, the A-space SNR is close to the K-edge subtraction value at low tube voltages but increases to approximately 3.5 times larger at 100 kV. The change may be due to the fact that for low voltages the peak of the tube spectrum is close to the K-edge energy while for larger voltages the signal includes the contributions of the difference in attenuation of soft tissue and gadolinium above the K-edge energy.

The larger SNR of the A-space method may seem surprising since the sharp discontinuity of the contrast material attenuation coefficient at the K-edge is markedly different from the background material attenuation coefficient. The superior SNR of the A-space method is due to the fact that the contrast material attenuation is different from the soft tissue not only at the K-edge energy but also throughout the range of energies in the x-ray tube spectrum. The A-space method measures this difference throughout the energy region

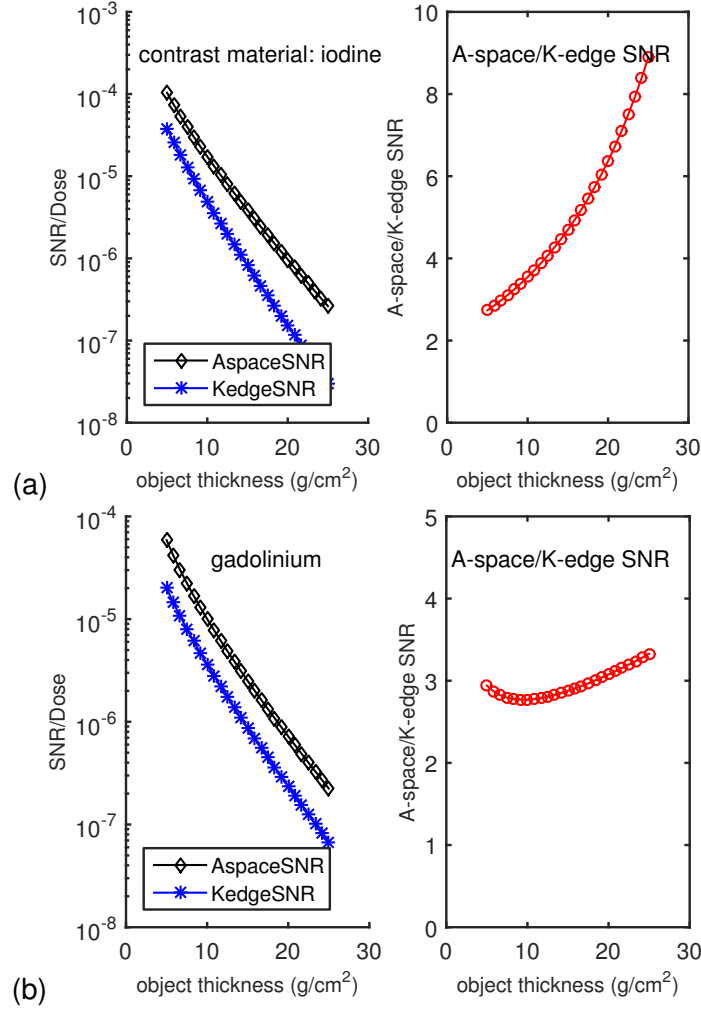


Figure 3.1: Contrast agent SNR per unit dose for K-edge and A-space methods as a function of object thickness for iodine (a) and gadolinium (b) containing contrast agents. For each material, the left panels shows the SNR per unit dose while the right panel shows the ratio of the SNR/dose. The tube voltage for the A-space method was 100 kV.

leading to larger signal. Also, the tube spectrum above the K-edge is attenuated less than at the K-edge leading to a lower noise measurement.

The K-edge method implementation in this study used idealized measurement spectra with high flux and energies tunable infinitesimally close to the K-edge energy. No sources with these characteristics that can be deployed to clinical institutions currently exist. Early work² used a broad spectrum x-ray tube source with a crystal monochromator but this did not provide a practical photon flux suitable for a clinical system. Other early work⁴ used an x-ray tube filtered by appropriately chosen materials. With this approach, there is a trade-off between the tube load-

ing and the width of the measurement spectra. For practical tube loading, the filtered spectra widths are not sufficiently small to give a large signal across the K-edge discontinuity. Another possibility¹³ is a synchrotron radiation source but currently this requires a large nuclear physics accelerator laboratory. There is research in “table-top” synchrotron radiation sources but these have not proved practical at this time. As shown by the results in this paper, even with an ideal monoenergetic source, the A-space method provides a better signal to noise ratio per dose.

The A-space method used in this study, although idealized, may be implementable in a clinical environment. X-ray tubes are widely used in diagnostic imag-

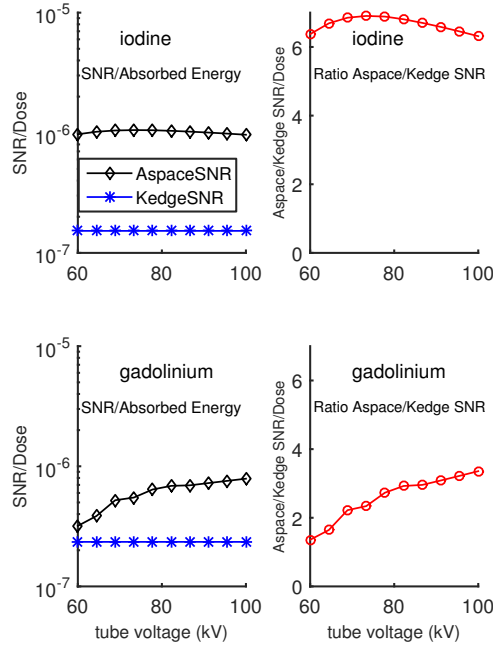


Figure 3.2: SNR per absorbed energy versus tube voltage. Iodine contrast in the top and gadolinium in the bottom panels. The K-edge method result does not depend on the tube spectrum so its SNR is constant. The panels on the right show the ratios of the SNRs. The object thickness was fixed at 20 g/cm^2 .

ing. The photon counting detector assumed negligible pileup and perfect PHA bins but realistic pileup and overlap between PHA bin responses may not substantially reduce the A-space method performance^{23,24}. The effect of photon counting detector imperfections on the SNR is a subject of current research.

5. CONCLUSION

The K-edge subtraction and the A-space method for imaging contrast agents containing iodine or gadolinium in a soft tissue background material are compared for their signal to noise ratio per unit dose. The A-space method has a better $SNR^2/dose$ for soft tissue object thicknesses from 10 to 25 g/cm^2 and for tube voltages above 60 kV.

6. Supplementary material

Matlab language code to reproduce the figures of this paper is available online¹.

References

- 1 R. Alvarez, "Matlab language software for paper: "K-edge subtraction vs. A-space processing for x-ray imaging of contrast agents: SNR"," July 2017. [Online]: <http://dx.doi.org/10.13140/RG.2.2.30400.64009>
- 2 B. Jacobson, "Dichromatic Absorption Radiography. Dichromography," *Acta Radiologica*, vol. Original Series, Volume 39, no. 6, pp. 437–452, Jun. 1953. [Online]: <http://tinyurl.com/JacobsonDichromatic1953>
- 3 P. Edholm and B. Jacobson, "Quantitative Determination of Iodine in Vivo," *Acta Radiologica*, vol. Original Series, Volume 52, no. 5, pp. 337–346, Nov. 1959. [Online]: <http://tinyurl.com/EdholmJacobson1959>
- 4 S. J. Riederer and C. A. Mistretta, "Selective iodine imaging using k-edge energies in computerized x-ray tomography," *Medical Physics*, vol. 4,

- no. 6, pp. 474–481, Nov. 1977. [Online]: <http://dx.doi.org/10.1118/1.594357>
- ⁵ R. E. Alvarez and A. Macovski, “Energy-selective reconstructions in X-ray computerized tomography,” *Phys. Med. Biol.*, vol. 21, pp. 733–44, 1976. [Online]: <http://dx.doi.org/10.1088/0031-9155/21/5/002>
- ⁶ R. E. Alvarez, “Near optimal energy selective x-ray imaging system performance with simple detectors,” *Med. Phys.*, vol. 37, pp. 822–841, 2010. [Online]: <http://tinyurl.com/NearOptimalEnergySelective>
- ⁷ M. J. Tapiovaara and R. Wagner, “SNR and DQE analysis of broad spectrum X-ray imaging,” *Phys. Med. Biol.*, vol. 30, pp. 519–529, 1985. [Online]: <http://doi.org/10.1088/0031-9155/30/6/002>
- ⁸ R. E. Alvarez, “Extraction of Energy Dependent Information in Radiography,” Ph.D. dissertation, Stanford University, 1976. [Online]: <http://www.dx.doi.org/10.13140/RG.2.2.12965.09446>
- ⁹ —, “Energy dependent information in x-ray imaging—part 1 the vector space description,” *Stanford University Information Systems Laboratory-unpublished*, 1982. [Online]: <http://dx.doi.org/10.13140/RG.2.2.19355.46887>
- ¹⁰ L. A. Lehmann, R. E. Alvarez, A. Macovski, W. R. Brody, N. J. Pelc, S. J. Riederer, and A. L. Hall, “Generalized image combinations in dual KVP digital radiography,” *Med. Phys.*, vol. 8, pp. 659–67, 1981.
- ¹¹ E. Roessl and R. Proksa, “K-edge imaging in x-ray computed tomography using multi-bin photon counting detectors,” *Phys. Med. Biol.*, vol. 52, pp. 4679–4696, 2007. [Online]: <http://dx.doi.org/10.1088/0031-9155/52/15/020>
- ¹² K. C. Zimmerman and T. Gilat Schmidt, “Comparison of quantitative K-edge empirical estimators using an energy-resolved photon-counting detector,” D. Kontos, T. G. Flohr, and J. Y. Lo, Eds., Mar. 2016, p. 97831S. [Online]: <http://dx.doi.org/10.1117/12.2217233>
- ¹³ F. A. Dilmanian, X. Y. Wu, E. C. Parsons, B. Ren, J. Kress, T. M. Button, L. D. Chapman, J. A. Coderre, F. Giron, D. Greenberg, D. J. Krus, Z. Liang, S. Marcovici, M. J. Petersen, C. T. Roque, M. Shleifer, D. N. Slatkin, W. C. Thomlinson, K. Yamamoto, and Z. Zhong, “Single- and dual-energy CT with monochromatic synchrotron x-rays,” *Phys. Med. Biol.*, vol. 42, no. 2, pp. 371–387, Feb. 1997. [Online]: <http://www.dx.doi.org/10.1088/0031-9155/42/2/009>
- ¹⁴ P. M. Shikhaliev, “Photon counting spectral CT: improved material decomposition with K-edge-filtered x-rays,” *Phys. Med Biol.*, vol. 57, no. 6, p. 1595, 2012. [Online]: <http://www.dx.doi.org/10.1088/0031-9155/57/6/1595>
- ¹⁵ H. Van Trees, K. Bell, and Z. Tian, *Detection Estimation and Modulation Theory, Detection, Estimation, and Filtering Theory*, ser. Detection Estimation and Modulation Theory. New York: Wiley, 2013. [Online]: <https://books.google.com/books?id=dnvaxqHDkbQC>
- ¹⁶ R. E. Alvarez, “Dimensionality and noise in energy selective x-ray imaging,” *Med. Phys.*, vol. 40, no. 11, p. 111909, 2013. [Online]: <http://dx.doi.org/10.1118/1.4824057>
- ¹⁷ R. E. Alvarez and E. J. Seppi, “A comparison of noise and dose in conventional and energy selective computed tomography,” *IEEE Trans. Nucl. Sci.*, vol. NS-26, pp. 2853–2856, 1979. [Online]: <http://www.dx.doi.org/10.1109/TNS.1979.4330549>
- ¹⁸ R. E. Alvarez, “Estimator for photon counting energy selective x-ray imaging with multi-bin pulse height analysis,” *Med. Phys.*, vol. 38, pp. 2324–2334, 2011. [Online]: <http://dx.doi.org/10.1118/1.3570658>

- ¹⁹ R. Alvarez, “Near optimal neural network estimator for spectral x-ray photon counting data with pileup,” *arXiv:1702.01006 [physics]*, Feb. 2017, arXiv: 1702.01006. [Online]: <http://arxiv.org/abs/1702.01006>
- ²⁰ S. M. Kay, *Fundamentals of Statistical Signal Processing, Volume I: Estimation Theory*. Upper Saddle River, NJ: Prentice Hall PTR, 1993, vol. Ch. 3.
- ²¹ “NIST: X-Ray Mass Attenuation Coefficients - Section 3.” [Online]: <https://physics.nist.gov/PhysRefData/XrayMassCoef/chap3.html>
- ²² J. M. Boone and J. A. Seibert, “An accurate method for computer-generating tungsten anode x-ray spectra from 30 to 140 kV,” *Med. Phys.*, vol. 24, pp. 1661–70, 1997. [Online]: <http://dx.doi.org/10.1118/1.597953>
- ²³ K. Taguchi and J. S. Iwanczyk, “Vision 20/20: Single photon counting x-ray detectors in medical imaging,” *Med. Phys.*, vol. 40, p. 100901, 2013. [Online]: <http://dx.doi.org/10.1118/1.4820371>
- ²⁴ R. E. Alvarez, “Signal to noise ratio of energy selective x-ray photon counting systems with pileup,” *Med. Phys.*, vol. 41, no. 11, p. 111909, 2014. [Online]: <http://dx.doi.org/10.1118/1.4898102>